

# First-principles derivation of vacuum surface energies from crystal structures

Marc Henry

*Institut Le Bel, University Louis Pasteur, 4, rue Blaise Pascal, 67070 Strasbourg cedex, France*

Received 19 March 2003; accepted 19 June 2003

## Abstract

Phase separation in solid state chemistry may occur following two main mechanisms. For high interfacial energy ( $\gamma \gg 0$ ), only local concentration fluctuations are allowed. Consequently, the new phase must first nucleate before growing up to a macroscopic scale (Classical Nucleation Theory or CNT). On the other hand, for vanishing interfacial energies ( $\gamma \sim 0$ ) macroscopic concentration fluctuations have a low energetic cost, and phase separation then leads to a deeply interconnected morphology (Spinodal Decomposition or SD). Consequently, it is very challenging to predict the order of magnitude of interfacial energies from the sole knowledge of the crystalline structure. Here we present a simple algorithm allowing to evaluate the vacuum surface energies of any crystalline material using a spherical charge approximation of density functional theory (DFT) equations and ab initio ground-state atomic properties. Using this formalism, it is easily explained why materials based on strong covalent bonds (oxides) or strong hydrogen bonds (ices) are expected to follow the CNT picture and why polymeric materials or metallic alloys prefer to undergo spontaneous SD. For materials displaying complex polymorphic behavior (such as observed for ice polymorphs), it becomes possible to find which polymorph should display the lowest surface energy and also to discriminate between correct and wrong crystallographic data. Thus we show for the first time that the reported crystal structure of ice-IV is characterized by a large *negative* surface energy and that it should be urgently revisited using accurate neutron diffraction data. Finally, we also demonstrate that the surface energy concept remains valid even at a molecular scale, bringing strong support to one of the most crucial hypothesis of CNT.

© 2003 Éditions scientifiques et médicales Elsevier SAS. All rights reserved.

The surface energy concept is found at the heart of many scientific fields such as surface chemistry (catalysis), mineralogy (ore flotation and crystallization), biology (capillary phenomena), polymer chemistry (paints and adhesives). Moreover, all colloidal phenomena concerning solids, such as wetting [1–3], nucleation [4] and crystal growth [5] or adhesion [6], also depend strongly on the relative values of surface tensions of solid–vapor or solid–liquid interfaces. Despite this widespread importance, numerical accesses to this crucial parameter remains quite elusive both from an experimental and theoretical point of view. In the following, we propose a new nonempirical computational way allowing to derive surface energy values directly from crystalline structures. The method being straightforward, cheap and reliable, it is hoped that it will be of some help to all scientists involved in colloidal and surface chemistry.

Our algorithm (nicknamed PACHA) is based on an electronegativity equalization principle based on a spherical charge approximation of density functional equations us-

ing universal spectroscopic electronegativities and ab initio atomic radii as atomic parameters [7]. Using this rigorous partition scheme of the electronic density between atoms, we have been able to derive a fully quantitative way of probing molecular interactions in the gaseous or crystalline state [8]. Other applications of the PACHA approach include accurate computation of H-atoms coordinates in hydrogen-bonded systems [8,9], prediction of  $pK_a$  values [9], molecular tectonics of polyoxometallate and silicate compounds [9,10] and fast computation of NMR tensors (chemical shifts and/or electrical field gradients) [11,12]. Briefly stated, we proceeded in the spirit of the Hellman–Feynman theorem, which shows that a consideration of classical electrostatic interactions suffices to determine the energy  $E$  of any physical system without the need for explicit inclusion of quantum-mechanical contributions [13]. Consequently, the total energy may always be partitioned as  $E = EB + F$ , with  $EB$  the classical electrostatic contribution (electrostatic balance) and  $F$ , the quantum-mechanical one. Let now  $C$  be a crystal characterized for one crystalline motif by  $E_C = EB_C + F_C$  and  $S$  a sphere of radius  $r$  extracted from this crystalline net-

*E-mail address:* [henry@chimie.u-strasbg.fr](mailto:henry@chimie.u-strasbg.fr).

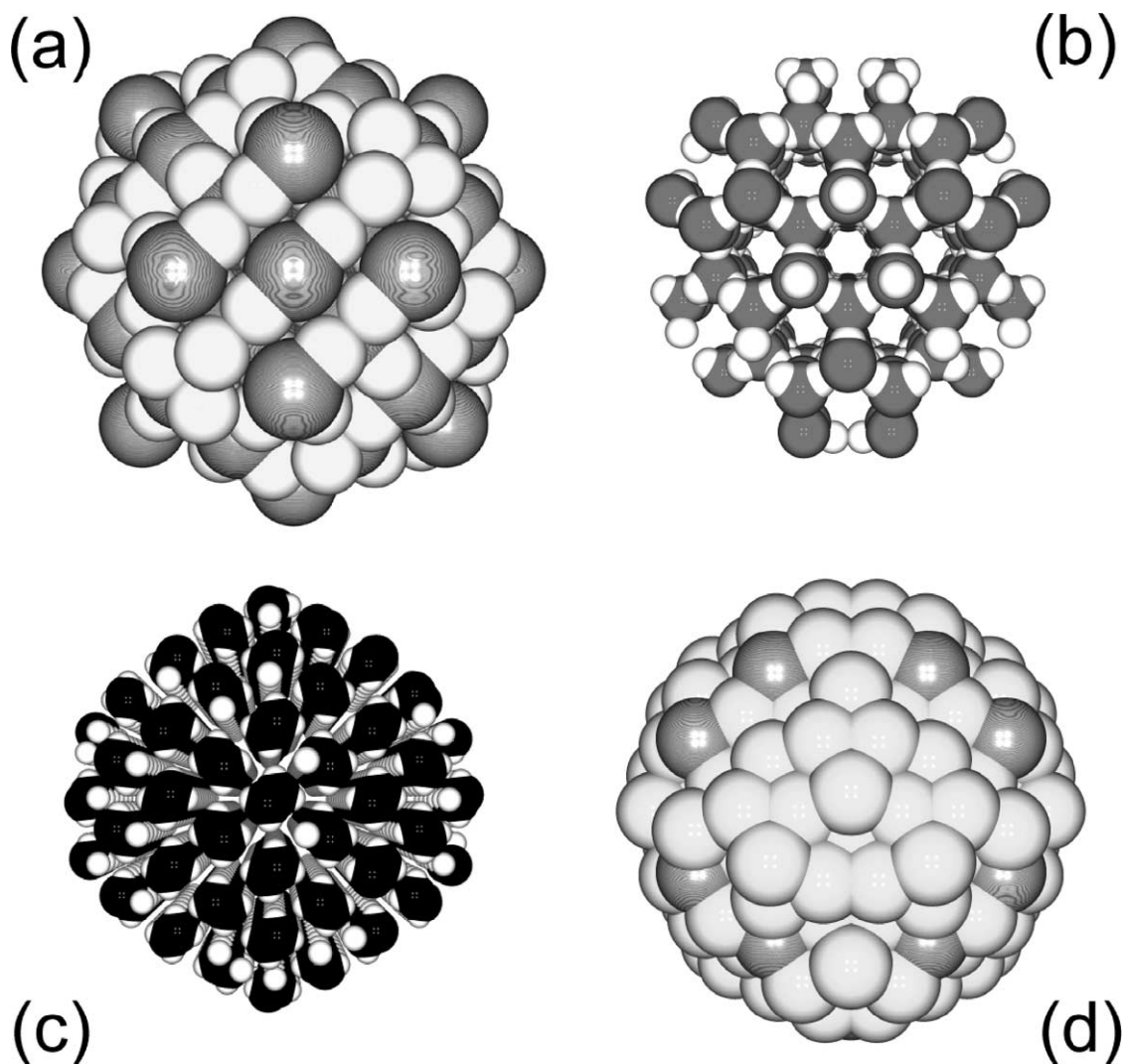


Fig. 1. Graphical overview of the materials concerned by this study. (a) A 1-nm rutile sphere containing 130  $\text{TiO}_2$  motifs and characterized by  $\gamma \sim 5.9 \text{ J m}^{-2}$ . (b) A 1-nm hexagonal ice sphere containing 132 water molecules and characterized by  $\gamma \sim 340 \text{ mJ m}^{-2}$ . (c) A 1.5-nm polyethylene sphere containing 650  $\text{CH}_2$  motifs and characterized by  $\gamma \sim +0.3 \text{ mJ m}^{-2}$ . (d) A 1.1-nm  $\text{Al}_6\text{Mn}$  sphere containing 52  $\text{Al}_6\text{Mn}$  motifs and characterized by  $\gamma \sim 14 \text{ mJ m}^{-2}$ .

work. If one thinks of  $S$  as a new system isolated in the vacuum, we should write as before  $E_S = EB_S + F_S$ . However, as  $S$  is a subsystem of  $C$  with exactly the same disposition of atoms and bonds, it is clear that  $F_S \sim n \times F_C$ , if  $n$  stands for the number of motifs found within the isolated sphere. From this sole assumption, it follows that the excess energy  $\Delta E = E_S - n \times E_C$  should scale like  $(EB_S - n \times EB_C)$  and that the corresponding surface energy  $\gamma$ , may be approximated in a quite straightforward way as

$$\gamma = \frac{EB_S - n \times EB_C}{4\pi r^2}. \quad (1)$$

Now, within a spherical charge approximation classical  $EB$ -terms are easily computed from the geometry (interatomic distances  $R_{ij}$ ) and partial charges distribution ( $eq_i$  and  $eq_j$ ) by a direct sum for the isolated sphere ( $M_{ij} = 1/R_{ij}$ ) or by an Ewald summation process for the crystal case (Madelung

matrix elements  $M_{ij}$ ) [7]

$$EB = \frac{e^2}{8\pi\epsilon_0} \sum_i \sum_j M_{ij} \times q_i q_j. \quad (2)$$

Finally, choosing eV-units for  $EB$ -values ( $1 \text{ eV} = 1.602 \times 10^{-16} \text{ mJ}$ ) and considering a sphere of radius  $r \text{ nm}$  ( $1 \text{ nm}^{-2} = 10^{18} \text{ m}^{-2}$ ), Eq. (1) becomes

$$\gamma (\text{mJ m}^{-2}) = 12.75 \times \frac{EB_S - n \times EB_C}{r^2}. \quad (3)$$

As stated above the simplicity of Eq. (3) allows us to investigate in a routine way the surface energy of any compound (organic, inorganic, polymeric or metallic) in the vacuum as soon as its crystalline structure is known.

Let us consider, for example, the case of the rutile structure displaying the  $\text{TiO}_2$  stoichiometry. This compound crystallizes in the tetragonal  $P4_2/mnm$  space group [14], characterized by  $EB_C = -23.421 \text{ eV/TiO}_2$  (see supplementary

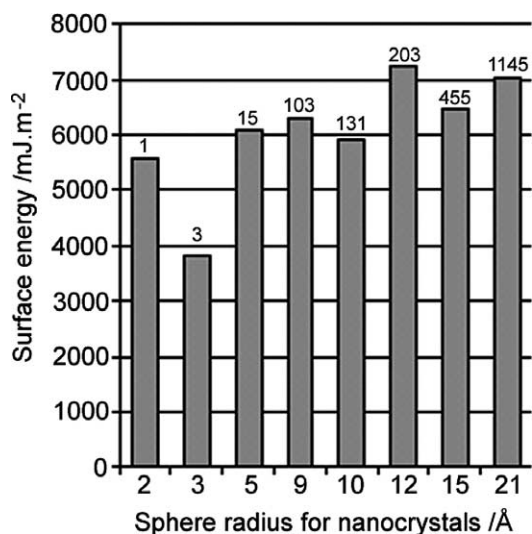


Fig. 2. Fluctuation around  $\gamma \sim 6 \text{ J m}^{-2}$  for nanosized rutile spheres. Numbers above bars refer to the  $n$ -value used in Eq. (3). Notice that even at a molecular scale ( $r = 0.2 \text{ nm}$ , just one linear O–Ti–O motif) one predicts that  $\gamma \sim 6 \text{ J m}^{-2}$ . The validity of the surface energy is accordingly a perfectly justified critical assumption of classical nucleation theory (CNT).

materials for computational details). From this crystal structure, it was also possible to generate a 1 nm-radius  $\text{TiO}_2$  sphere displaying the  $\text{Ti}_{131}\text{O}_{266}$  stoichiometry ( $n = 131$ ) and characterized by  $EB_S = -2603.234 \text{ eV}$  (Fig. 1a). Inserting these values in Eq. (3) immediately leads to  $\gamma(\text{rutile}) = 5.9 \text{ J m}^{-2}$ . However, as evidenced in Eq. (3) this value has been computed for a very particular size  $r$  of the particle extracted from the network. One may then wonder what result would be obtained for larger or smaller nanocrystals. As shown in Fig. 2, the surface energy does not change very much when  $r$  changes from 0.2 nm (just one  $\text{TiO}_2$  motif or  $n = 1$ ) to 2 nm ( $n = 1145$ ). This is an important result as one of the basic assumption of classical nucleation theory (CNT) is the persistence of the surface energy concept down to molecular sizes. Here we have a direct proof of the validity of this assumption. The small fluctuations ( $\sim 20\%$ ) observed in Fig. 2 around the value  $\gamma \sim 6.0 \text{ J m}^{-2}$  are obviously related to the well-known dependence of the surface energy as a function of the Miller indexes ( $h, k, l$ ) of the various reticular planes characterizing the rutile structure. As we are considering spheres embracing not just one but several reticular planes (see Fig. 1), and as the relative proportion of each kind of plane depends on the sphere size, small variations around a mean value are expected. This demonstrates again the usefulness of our approach, as in a real nanocrystal, several reticular planes are expected to contribute to the total surface energy.

It is quite remarkable that the number  $\gamma \sim 6.0 \text{ J m}^{-2}$  was derived directly from the rutile crystal structure using just ab initio ground state atomic properties (configuration energies and valence orbital atomic radii) expressed within the spherical charge approximation of DFT equations. This value has thus an absolute character independent of any

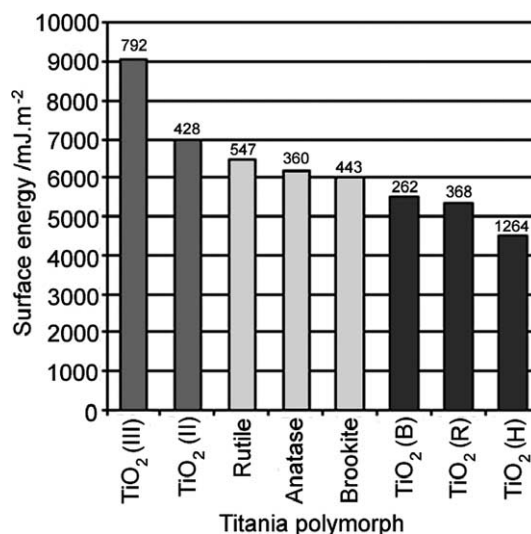


Fig. 3. Classification of the eight  $\text{TiO}_2$  polymorphs according to decreasing surface energy.  $\text{TiO}_2$  (III) is the polymorph stable above 12 GPa (baddeleyite structure).  $\text{TiO}_2$  (II) is the polymorph stable at  $T = 450 \text{ }^\circ\text{C}$  and  $P = 400 \text{ MPa}$  ( $\alpha\text{-PbO}_2$  structure).  $\text{TiO}_2$  (B) is the phase obtained by topotactic water removal from layered titanates  $\text{Na}_2\text{Ti}_n\text{O}_{2n+1}$ .  $\text{TiO}_2$  (R) is the phase obtained by topotactic oxidation of  $\text{Li}_x\text{TiO}_2$  bronzes (ramsdellite structure).  $\text{TiO}_2$  (H) is the phase obtained by topotactic oxidation of  $\text{K}_x\text{TiO}_2$  bronzes (hollandite structure). Rutile, anatase and brookite are the three naturally occurring titania polymorphs. Numbers above bars refer to standard deviations observed for three computations ( $r \sim 0.9, 1$  and  $1.1 \text{ nm}$ ).

feeling about the kind of chemical bonding at work in the rutile structure. This number is fixed by Nature itself and not by our preconceived ideas about ionic or covalent bonding. Moreover, it is an intrinsic vacuum property of the rutile structure independent of any adsorbed species or surface relaxation effects. This is also why it is significantly higher than theoretical values derived after surface relaxation which lead to  $\gamma \sim 2.0 \text{ J m}^{-2}$  for the (001) planes,  $\gamma \sim 1.4 \text{ J m}^{-2}$  for the (100) planes and  $\gamma \sim 1.1 \text{ J m}^{-2}$  for the (110) planes [15]. These values are themselves much higher than experimental values  $\gamma \sim 270 \text{ mJ m}^{-2}$  derived from CNT in aqueous solutions [16], where adsorption of solute species (characterized by their chemical potential  $\mu$ ) on vacant sites (characterized by their density  $\Gamma$ ) allows a further reduction of these surface energies according to the Gibbs formula  $d\gamma = -\Gamma \times d\mu$ . Consequently, even with these severe limitations (nonrelaxed surfaces under strict vacuum conditions), we have in hand a very useful tool to probe in an ab initio way surface energy as a function of atomic spatial dispositions.

This could be easily demonstrated in the case of titanium oxides by considering other titania polymorphs (see Fig. 3 and supporting information for computational details). All values have been computed for nanosized spheres and correspond to averages over three calculations made for  $r \sim 0.9, 1.0$  and  $1.1 \text{ nm}$ . For each case, the size has been slightly adjusted in order to get an almost electrically neutral stoichiometry  $(\text{TiO}_2)_n$ . It is then found that the surface energy is approximately doubled on going from

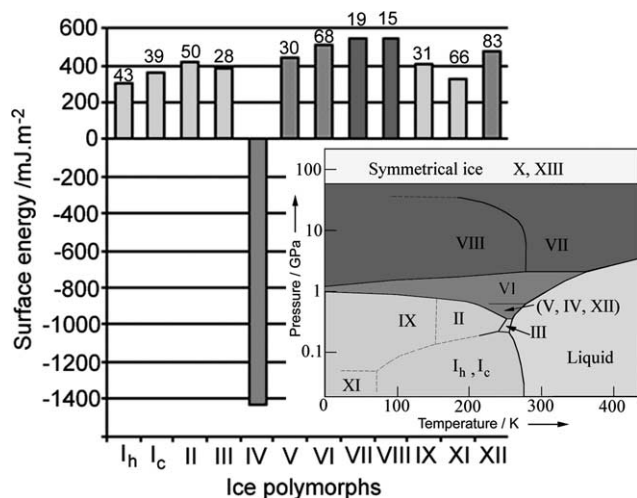


Fig. 4. Phase diagram and surface energies for the twelve known ice polymorphs. Notice that hexagonal ice displays the lowest surface energy and the large negative value found for the ice-IV polymorph indicating problems in single-crystal X-ray data. Numbers above bars refer to standard deviations observed for three computations ( $r \sim 0.9, 1$  and  $1.1$  nm).

the most opened polymorph (hollandite-type with  $\gamma \sim 4.5 \text{ J m}^{-2}$ ) to the most compact one (baddeleyite-type with  $\gamma \sim 9.1 \text{ J m}^{-2}$ ). Consequently, it seems that surface energy has a direct correlation with crystalline density. Among the three most common occurring titania polymorphs we found the following order: brookite ( $\gamma \sim 6.0 \text{ J m}^{-2}$ ) < anatase ( $\gamma \sim 6.2 \text{ J m}^{-2}$ ) < rutile ( $\gamma \sim 6.5 \text{ J m}^{-2}$ ). Let us, however, recall that these are mean values and that according to the reported standard deviations (values at the top of the stick diagram in Fig. 3), other orders may be found depending on the kind of reticular planes exposed on the surface.

Another interesting aspect of this new approaches to the evaluation of surface energies lies in the fact that any kind of crystal can be investigated. In the previous case, we have considered an oxide with a rather high melting point ( $\sim 1850^\circ\text{C}$ ) and it was thus not quite surprising to find surface energies well above  $1 \text{ J m}^{-2}$ . These high values just reflect the considerable strength of Ti–O bonds. We may now have a look at another kind of crystalline oxide network, with a much lower melting point and thus displaying weaker bonds. A typical example is provided by the twelve ice polymorphs which have been thoroughly previously studied from a bond energy standpoint [8]. Two main points have to be checked in order to validate our *ab initio* approach. First, it is well known that H-bond strengths are about 20 times weaker than covalent ones. Consequently, one may expect that surface energies of H-bonded oxides (ices) should be roughly 20 times smaller than that of metallic oxides such as  $\text{TiO}_2$ . Second, owing to its widespread occurrence in Nature, the hexagonal polymorph ( $I_h$ ) should be the one displaying the lowest surface energy. Fig. 4 shows the results obtained applying Eq. (3) to all currently known ice polymorphs. As expected, the phase displaying the lowest surface energy is hexagonal ice  $I_h$  characterized by  $\gamma = 298(43) \text{ mJ m}^{-2}$ . This value computed from first principles in vacuum and with

nonrelaxed surfaces is as expected larger than the interfacial energy usually quoted [17] for the ice/steam interface:  $70 \text{ mJ m}^{-2} < \gamma_{iv} < 110 \text{ mJ m}^{-2}$ . As for the rutile surface energy, one may then conclude that surface relaxation and water adsorption accounts for a threefold decrease in the surface energy. Another interesting point is that with  $\gamma = 322(66) \text{ mJ m}^{-2}$ , ice-XI display a lower surface energy than ice  $I_c$  which is characterized by  $\gamma = 359(39) \text{ mJ m}^{-2}$ . As expected the two high-pressure polymorphs ice-VII and ice-VIII display the highest values of surface energies:  $\gamma \sim 550(20) \text{ mJ m}^{-2}$ . Other polymorphs display intermediate values, with one notable exception, ice-IV, characterized by a large negative surface energy  $\gamma < -1000 \text{ mJ m}^{-2}$ . At first sight this value may seem quite surprising, as it means that a nanosized crystal of ice-IV should be much more stable than the whole macroscopic crystalline lattice. However, let us recall that ice-IV is the only ice-polymorph characterized by a positive (i.e., repulsive) H-bond energy:  $E_{HB} = +51(55) \text{ kJ mol}^{-1}$  ( $E_{HB}$  was found to be less than  $-15 \text{ kJ mol}^{-1}$  for all other known ice polymorphs) [8]. The negative surface energy computed for the ice-IV network is just a clear evidence that the reported single-crystal X-ray diffraction structure has something wrong. Consequently, we are in position to predict, that when neutron diffraction data would be available for ice-IV, a negative H-bond energy and a positive surface energy would be found using our computational scheme to the new structure.

Another critical test for our theory is to consider crystals where cohesive energy is provided by weak van der Waals interactions. As these interactions are about ten times smaller than H-bond interactions, it may be expected that these crystals should be characterized by very small surface energies. As shown in Fig. 5, referring to polyethylene crystals  $(\text{CH}_2)_n$ , this is indeed the case as such a material is characterized by  $\gamma < 10 \text{ mJ m}^{-2}$  over a wide size range (0.2–2 nm). A noticeable feature in Fig. 5 is that for some particular sizes the surface energy may be zero or even slightly negative. In deep contrast with the crystal structure of ice-IV, one may assume that the crystal data is here basically correct and that negative values comes from truncation errors in the difference between two numbers displaying the same order of magnitude whatever the size of the sphere may be. In fact, taking the average over Fig. 5 leads to  $\gamma = -0.6(4) \text{ mJ m}^{-2}$ , i.e., one may safely assume that  $\gamma \sim 0$  for such apolar polymeric materials. The direct consequence of this matter of fact, is a first-principles proof that polymeric solid state chemistry should be governed by spinodal decomposition processes, as composition fluctuations over macroscopic distances are possible only when  $\gamma \sim 0$ . In contrast, covalent or hydrogen-bond solid state chemistry should be rather governed by nucleation-growth processes, as only local fluctuations in composition are allowed when  $\gamma \gg 0$ . This fundamental experimental partition for phase separation phenomena then acquires here a firm theoretical basis. It also provides a final decisive test for our approach as it is well known that spinodal decomposition processes

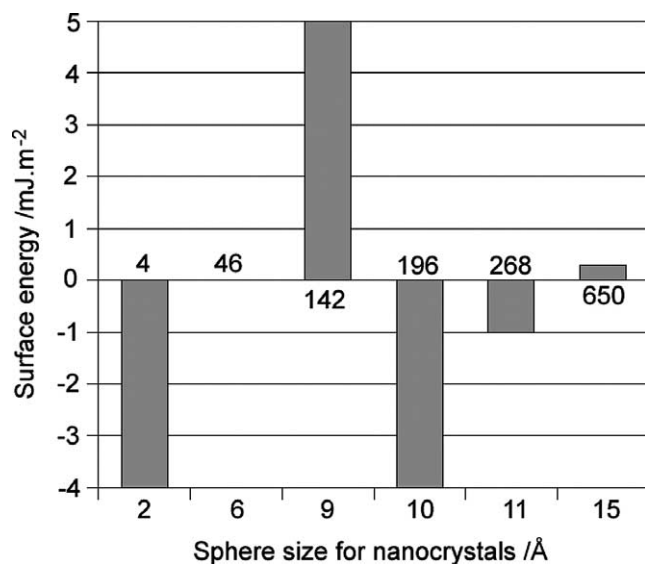


Fig. 5. Fluctuations around  $\gamma \sim 0 \text{ mJ m}^{-2}$  for nanosized polyethylene spheres. Numbers below bars refer to the  $n$ -value used in Eq. (3). Notice that the surface energy exactly vanishes for  $r = 6 \text{ \AA}$ . A vanishing surface energy just means that the thermodynamic barrier separating a nanocrystal from a macroscopic crystal has disappeared. Consequently, interconnected patterns characteristic of spinodal decomposition processes (diffuse interfaces) becomes competitive against isolated nucleation/growth pattern (sharp interfaces).

may be encountered in another class of materials very different from polymers, namely, metallic alloys. From the above analysis, it follows that surface energy of metallic alloys should be definitively positive as metallic bonds are stronger than van der Waals bonds, but it should remain nevertheless quite low ( $\sim 10 \text{ mJ m}^{-2}$ ) to allow composition fluctuations over large distances (spinodal decomposition). For example, there is some experimental evidence [18] that the interfacial energy between icosahedral  $\text{Al}_{86}\text{Mn}_{14}$  alloys and crystalline  $\text{Al}_6\text{Mn}$  phases was only  $30 \text{ mJ m}^{-2}$ . Using the recently redetermined [19] crystal structure of  $\text{Al}_6\text{Mn}$ , we have accordingly found applying Eq. (3) to nanometer-sized crystalline spheres (Fig. 1d),  $\gamma = 17(4) \text{ mJ m}^{-2}$ . Again, we get

the right order of magnitude of the surface energy without the explicit knowledge that we are considering a metallic alloy and not a polymeric of a hydrogen-bonded network. This definitively demonstrates the universality of Eq. (3) and the sound physical basis of the spherical charge approximation of DFT equations using ab initio ground-state atomic properties [7]. In fact, the only case where our approach is useless concerns the case of crystalline elements (unary compounds such as diamond versus graphite structures or ccp versus hcp metals). In these cases explicit consideration of quantum-mechanical interactions are absolutely needed, owing to the lack of polarity linked to the vanishing electronegativity differences among the various nonequivalent crystallographic sites. In all other cases, Eq. (3) may be routinely used to get a reasonable upper limit (unrelaxed vacuum interfaces) to the surface energy of any crystalline material.

## References

- [1] P.G. de Gennes, *Rev. Mod. Phys.* 57 (1985) 827.
- [2] D.Y. Kwok, A.W. Neumann, *Prog. Colloid Polym. Sci.* 109 (1998) 170.
- [3] J.M. Douillard, V. Médout-Marère, *J. Colloid Interface Sci.* 223 (2000) 255.
- [4] A.E. Nielsen, O. Söhnel, *J. Cryst. Growth* 11 (1971) 233.
- [5] J. Hulliger, *Angew. Chem., Int. Ed. Engl.* 33 (1994) 143.
- [6] P.G. de Gennes, *Nature* 412 (2001) 385.
- [7] M. Henry, *Chem. Phys. Chem.* 3 (2002) 561.
- [8] M. Henry, *Chem. Phys. Chem.* 3 (2002) 607.
- [9] M. Henry, *J. Cluster Sci.* 13 (2002) 437.
- [10] M. Henry, *Coord. Chem. Rev.* 180 (1998) 1109.
- [11] T.M. Alam, M. Henry, *Phys. Chem. Chem. Phys.* 2 (2000) 23.
- [12] M. Henry, *ACS Symp. Ser.* 732 (1999) 277.
- [13] P.P. Politzer, H. Weinstein, *J. Chem. Phys.* 71 (1979) 4218.
- [14] R. Restori, D. Schwarzenbach, J.R. Schneider, *Acta Crystallogr. B* 39 (1987) 251.
- [15] V. Swamy, J. Muscat, J.D. Gale, N.M. Harrison, *Surf. Sci.* 504 (2002) 115.
- [16] O. Söhnel, *Collect. Czech. Chem. Commun.* 40 (1975) 2560.
- [17] L. Makkonen, *J. Phys. Chem. B* 101 (1997) 6196.
- [18] K.F. Kelton, J.C. Holzer, *Phys. Rev. B* 37 (1988) 3940.
- [19] K. Yamamoto, Y. Matsuo, *J. Phys. C: Condens. Matter* 12 (2000) 2359.